Molecular Vision **1998; 4:19** <http://www.molvis.org/molvis/v4/p19>
Received 14 July 1997 | Accepted 21 September 1998 | Published 29 September 1998

Structural Features of the Aldose Reductase and Aldehyde Reductase Inhibitor-Binding Sites

Ossama El-Kabbani,[1] David K. Wilson,[2] J. Mark Petrash,[3] Florante A. Quiocho[2]

[1]Department of Medicinal Chemistry, Victorian College of Pharmacy, Monash University, Parkville, Vic 3052, Australia; [2]Howard Hughes Medical Institute and Department of Biochemistry, Baylor College of Medicine, Houston, TX, USA; [3]Department of Ophthalmology and Visual Sciences, Washington University School of Medicine, St. Louis, MO, USA

The three-dimensional structures of aldose reductase and aldehyde reductase, members of the aldo-keto reductase superfamily, are composed of similar α/β TIM-barrels. However, examination of the structures reveals that the inhibitor-binding site of aldose reductase differs from that of aldehyde reductase due to the participation of non-conserved residues in its formation. This information will be useful in the design of inhibitors to prevent or delay diabetic retinopathy. A review of the structures of the inhibitor-binding sites is presented.

The aldo-keto reductases (AKR) comprise a superfamily of M_r ~36,000 proteins that catalyze the reduction of a wide variety of substrates including aliphatic and polycyclic aldehydes, aldoses, lipid-derived aldehydes, and xenobiotics. Some AKRs have been shown to catalyze key steps in diverse metabolic pathways such as prostaglandin [1] and steroid [2,3] synthesis. However, in most cases the beneficial roles fulfilled by individual AKRs are not known. Most AKRs demonstrate overlapping specificity for various structural classes of substrates, a situation that has led to much confusion in the literature. The recently proposed nomenclature system for the AKR superfamily, which is based on systematic comparisons of primary sequences, may help to clarify the relationships among members of this expanding group of proteins [4]. An AKR Superfamily web site has been set up as a resource to investigators interested in receiving and adding sequence data to the AKR database.

Aldose reductase (ALR2) is one of the most thoroughly studied of the aldo-keto reductases due to its putative involvement in the pathogenesis of diabetic eye disease [5]. ALR2 catalyzes the NADPH-dependent reduction of glucose to sorbitol, the first step of the sorbitol pathway (Figure 1). The pathway is completed by sorbitol dehydrogenase, which catalyzes the NAD^+-dependent oxidation of sorbitol to fructose. A large body of evidence, derived principally from experimental animal studies, supports the hypothesis that enhanced metabolism of glucose through the polyol pathway results in biochemical imbalances associated with diabetic complications. Chronic hyperglycemia leads to many changes in target tissues of diabetes including accumulation of excess polyol, alteration in the relative abundance of oxidized and reduced nicotinamide coenzymes, changes in the levels of glycolytic intermediates and loss of myoinositol and glutathione [6]. Since many of these biochemical alterations appear to be derived from accelerated flux of glucose through the sorbitol pathway, ALR2 inhibition represents an attractive strategy for prevention of diabetic complications. The beneficial effect of aldose reductase inhibitors (ARIs) in preventing or substantially delaying the onset of diabetic complications in experimental models provides strong support to this hypothesis. Moreover, transgenic animal studies have shown that over-expression of ALR2 confers an increased susceptibility to diabetic cataract [7] and morphological changes in the retinal vasculature similar to those observed in human diabetic retinopathy [8]. Examples of ARIs are shown in Figure 2.

Correspondence to: Ossama El-Kabbani, Ph.D., Department of Medicinal Chemistry, Victorian College of Pharmacy, Monash University (Parkville Campus), 381 Royal Parade, Parkville, Vic 3052, Australia; Phone: 61 3 9903 9691; Fax: 61 3 9903 9582; email: ossama.el-kabbani@vcp.monash.edu.au

Structural features of the AKR active site

X-ray crystallography and site directed mutagenesis studies have provided important insight into the structures and catalytic mechanisms of several AKRs. Crystallographic analyses of ALR2 (PDB entry 1mar) [9,10], aldehyde reductase (ALR1, PDB entry 1ae4) [11-14], a fibroblast growth factor induced protein (FR-1, PDB entry 1frb) [15], and 3α-hydroxysteroid dehydrogenase (3α-HSD, PDB entry 1ral) [16] have shown that the three-dimensional structures are composed of similar α/β TIM-barrels. The three-dimensional structure of ALR2 is shown in Figure 3. ALR2 folds into an α/β-barrel with a core of eight parallel β-strands. Adjacent strands are connected by eight parallel α-helical segments running antiparallel to the β-sheet. The active site is located at the C-terminal end of the β-barrel. The symmetry of the TIM-barrel is disrupted by the presence of two short antiparallel β-strands at the N-terminus connected by a tight turn closing the bottom of the barrel, three large exposed loops partially covering the top of the barrel, and two α-helices. Based on the crystal structures, the proposed catalytic mechanism of the AKRs consists of a stereospecific transfer of the 4-*pro-R* hydrogen from the exposed C-4 of the nicotinamide of the bound NADPH to the carbon of the carbonyl group of the substrate, followed by the protonation of the substrate carbonyl oxygen by a proton donor group. The hydroxyl group of a conserved residue, Tyr 50 (the sequence numbering of ALR1 [11] is used)

is within van der Waals contacts (<4.0 angstroms) with the C-4 of the nicotinamide. The hydrogen-bond interaction between the hydroxyl group of Tyr 50 and the ammonium side-chain of Lys 80, which in turn forms a salt bridge with Asp 45, facilitates the proton transfer. However, a histidine residue has also been implicated in the catalytic mechanism [17]. In ALR2 and 3α-HSD, site-directed mutagenesis studies have concluded that Tyr 50 is the proton donor and that His 113 is involved in substrate recognition [18-20]. The reaction catalyzed by ALR1 and ALR2 proceeds through an ordered sequential kinetic mechanism with NADPH binding first and $NADP^+$ being released last [21,22]. The Asp 45-Lys 80-Tyr 50 system maintains an overall neutral charge on the enzyme's active site between pH 6-8, allowing a proton to be transferred to the carbonyl oxygen of the substrate and a negative charge to develop on the tyrosyl hydroxide.

Despite an overall similarity in the AKRs structures and mechanisms, differences in the structure and function of active site residues in the enzymes have been demonstrated by X-ray crystallography [12,14], molecular modeling [13], and site-directed mutagenesis [14,23]. The structure of the active site of ALR1 differs significantly from that of ALR2, FR-1, and 3α-HSD due to the participation of an eight-residue insertion segment from the C-terminal loop (Asp 306, Gly 307, Lys 308, Arg 309, Val 310, Pro 311, Arg 312, and Asp 313) lining the active site pocket (Figure 4) [13,14]. Moreover, a recent study using site-directed mutagenesis has identified the non-conserved Arg 312 as the residue responsible for the carboxyl-containing substrate preference of ALR1 [23]. A number of recent enzyme structure-function studies have been attempted to define the interactions between ALR1 and ALR2 and the various classes of ARIs with the intention of facilitating structure-based drug design and improving inhibitor potency and specificity [24-26]. X-ray crystallographic studies have shown that the inhibitors tolrestat and zopolrestat bind in the active sites of ALR1 [14] and ALR2 [10], respectively. Mutation of the human ALR2 active site residues, Tyr 50 to Phe (or His) and Trp 22 to Ala, greatly influences the inhibitory activity of ARIs [18]. In ALR1, mutation of residues involved in lining the active site pocket (the conserved His 113 to Gln or the non-conserved Arg 312 to Ala) alters the potency of inhibition of the enzyme with ARIs, suggesting that enzyme inhibition is a consequence of the interactions between the inhibitor and the active site of the enzyme [14,23,26].

In previous studies, we have compared the NADPH-binding site of ALR2 with that of ALR1 [12] and FR-1 [15], and we have shown that the coenzyme-binding site is the same for ALR1, ALR2, and FR-1 (Figure 5). The coenzyme is bound in an extended conformation with the nicotinamide moiety forming part of the base of the active site cavity. The pyrophosphate bridge of NADPH is tied down by loop B (residues 214-230) which holds NADPH tightly in place. While NADPH binds to ALR1, ALR2, and FR-1, ALR2 and FR-1 have a higher affinity for NADPH compared to ALR1 [15,22,27] (K_d of 0.16 μM, 0.45 μM and 1.6 μM, respectively). The ring of the nicotinamide is oriented so that the 4-*pro*-*R* hydrogen is directed toward the opening of the active site pocket. This orientation is maintained by several interactions: the stacking of the A face of the nicotinamide ring against Tyr 210 located at the bottom of the active site pocket and the hydrogen bonding of the amide group of the nicotinamide group with Gln 184, Asn 163, and Ser 162. The interactions that favor the binding of NADPH over NADH are also conserved; Lys 263 and Arg 269 are salt linked to the 2'-phosphate of the adenosine moiety of NADPH.

The ternary structures of ALR1 [14], ALR2 [10], and FR-1 [15] in complex with coenzyme and inhibitor have recently been determined. The active sites of ALR2 and FR-1 are occupied in a very similar manner by the inhibitor zopolrestat [15]. Here, we compare the structure of the inhibitor-binding site of ALR1 with that of ALR2 and indicate reasons for the differences in the potency of inhibition by ARIs.

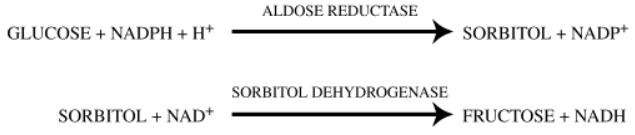

Figure 1. The polyol pathway. Aldose reductase, the first and rate limiting enzyme of the polyol pathway, catalyzes the NADPH-dependent reduction of glucose to sorbitol. The pathway is completed by the second enzyme of the polyol pathway, sorbitol dehydrogenase, which converts sorbitol to fructose.

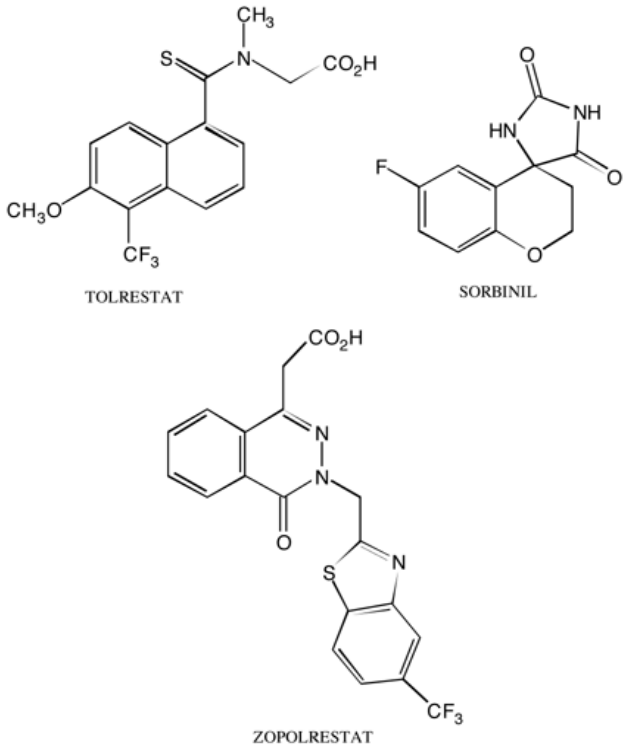

Figure 2. Schematic diagram of ARI structures. Spirohydantoins (*e. g.* sorbinil) and carboxylic acids (*e. g.* tolrestat and zopolrestat) represent two major classes of aldose reductase inhibitors. Our recent crystallographic studies have revealed that tolrestat and zopolrestat bind ALR1 and ALR2, respectively, at the active site.

Differences in ALR1 and ALR2 structures

The high degree of homology that exists between the primary structures of porcine ALR1 and human ALR2 (51% sequence identity [11]) is also reflected in their tertiary structures. The main-chain atoms (excluding the loop regions) from the porcine ALR1 molecule superimpose on the corresponding atoms from human ALR2 with a root-mean-square deviation of 0.87 angstrom (Figure 4). The main-chain atoms that deviate the most (>1.0 angstrom) belong to residues present on the surface of the molecules, while the main-chain atoms of the core β-sheet deviate the least among the two structures. The active site is located at the C-terminal end of the β-barrel and exists in a region with the least conserved residues [11]. A major difference is the participation of the eight-residue insertion segment from the C-terminal loop of ALR1 (residues 306-313) in lining the active site pocket. Despite an overall homology in sequence and structure of ALR1 and ALR2, antiserum to ALR1 does not cross react with ALR2 [28]. The differences in sequence and structure of the C-terminal loop in ALR1 and ALR2 may account for the lack of immunological cross reactivity between the two enzymes.

Differences in ALR1 and ALR2 inhibitor-binding sites

Inhibition and binding studies have suggested that ARIs are uncompetitive or non-competitive inhibitors in the forward direction of the reaction [29]. However, we have recently demonstrated using X-ray crystallography that two carboxylic acid inhibitors, tolrestat and zopolrestat, bind at the active sites of ALR1 [14] and ALR2 [10], respectively. Zopolrestat and tolrestat display IC_{50} values of 27 μM and 0.72 μM with human ALR1 (porcine and human ALR1 exhibit 93% sequence identity [11]), and 0.06 μM and 0.01 μM with human ALR2, respectively [26]. The fitted inhibitors occupy almost the entire active site pockets of the enzymes (Figure 6). Four of the nine hydrogen bonds present between ALR2 and zopolrestat are conserved in the ALR1-tolrestat structure. The side-chains of Tyr 50, His 113, and Trp 114 are within hydrogen bonding distance of the carboxylate group of tolrestat. In the ALR2-zopolrestat structure the N2 of the phthalazinone ring and the N3 of the benzothiazole ring of the inhibitor are hydrogen bonded to the SH group of Cys 299 and the backbone NH group of Leu 301, respectively. The residues corresponding to Cys 299 and Leu 301 in ALR1, Ile 299 and Pro 301, can not form a hydrogen bond with the inhibitor. The trifluoromethyl group of zopolrestat is hydrogen bonded to the OH group of Thr 116 of ALR2. In ALR1, however, Tyr 116, the residue corresponding to Thr 116 of ALR2, is not within hydrogen bonding distance with the trifluoromethyl group of tolrestat. In the FR-1 ternary complex structure the thiol group of Cys 299 and the amide main-chain nitrogen of Leu 301, which donate hydrogen bonds to zopolrestat bound in ALR2, have been replaced by water molecules [15]. In addition, similar to ALR1, none of the fluorine atoms of inhibitor accepts a hydrogen bond in the FR-1 ternary complex structure [15].

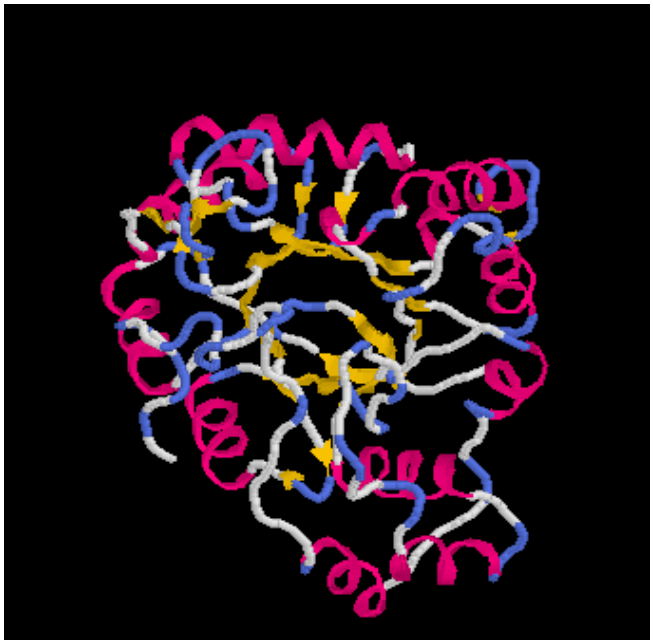

Figure 3. TIM-barrel structure of ALR2. A representative frame of a movie shows the backbone folding of ALR2. The ribbons in magenta show eight α-helices surrounding a core of eight β-strands (in yellow) all in parallel orientation. The arrows on the β-strands point from N- to C-terminus. The active site is located on the C-terminal side of the β-strands and is associated with three loops (in white and blue). The quicktime movie can be viewed at http://www.molvis.org/molvis/v4/p19.

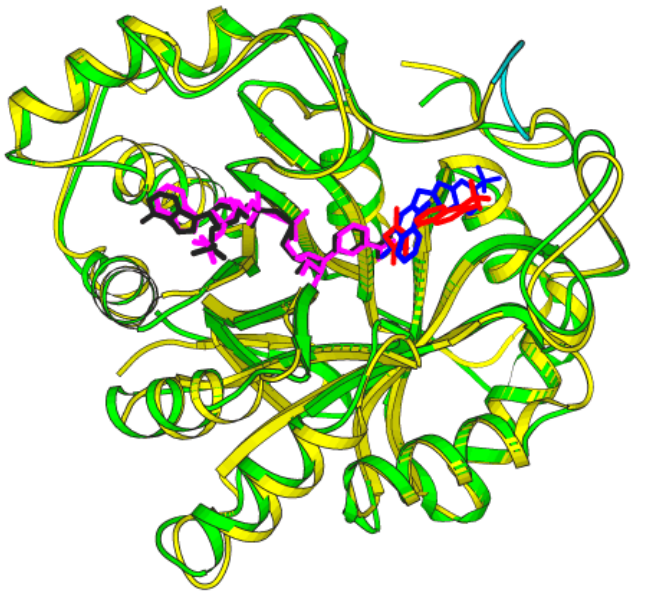

Figure 4. Backbone foldings of ALR1 and ALR2. Superposition of porcine ALR1-tolrestat (back bone in yellow, coenzyme in pink, inhibitor in red) and human ALR2-zopolrestat (back bone in green, coenzyme in black, inhibitor in blue) structures. The eight residue insertion segment in the C-terminal loop of ALR1 (residues 306-313) is shown in cyan. Ribbon drawings were prepared using MOLSCRIPT [37].

A major difference that exists between the structures of the inhibitor-binding site of ALR1 and ALR2 is the participation of the non-conserved Arg 312 and Asp 313 of ALR1 in lining the inhibitor-binding site [14] (Figure 6). Upon binding of tolrestat to ALR1, the side-chain of Arg 312 moves to accommodate the inhibitor in the active site pocket and is positioned within van der Waals contacts with the trifluoromethyl group of the inhibitor [14]. Mutation of Arg 312 to Ala reduces the value of the binding constant for both tolrestat and zopolrestat in the forward direction, thus enabling the inhibitor to bind more tightly [14]. Tolrestat and zopolrestat are 130 and 24 fold, respectively, more potent inhibitors of R312A than the wild type ALR1 [14]. This would be expected given that Arg 312 is not present in the active site of ALR2 and mutation of this residue to Ala in ALR1 makes the ALR1 active site more similar to that of ALR2 in this respect.

Superpositioning of the ternary complex structures of ALR1 and ALR2 shows that the *N*-methylthioamide group of tolrestat is positioned approximately in the plane of the phthalazinone ring of zopolrestat while the plane of the naphthalene ring intersects with the benzothiazole ring (Figure 6). The carboxylate oxygen of the inhibitors mimic the carbonyl oxygen of the substrate and are within van der Waals contacts with the hydroxyl group of Tyr 50, the proton donor [9,12]. The carboxylate carbon is within van der Waals contacts with the C-4 of the nicotinamide ring of the coenzyme (<4.0 angstroms), mimicking the carbon in a substrate that accepts the hydride during enzymatic reaction. In ALR2, eleven apolar residues that line the active site pocket are involved in van der Waals contacts with zopolrestat (Trp 22, Tyr 50, Trp 82, Trp 114, Phe 118, Phe 125, Trp 220, Ala 300, Leu 301, Tyr 319, and Pro 320), consistent with the observation that aromatic compounds are the best substrates for the enzyme [30]. The corresponding residues in ALR1 are: Trp 22, Tyr 50, Trp 82, Trp 114, Phe 118, Phe 125, Trp 220, Val 300, Pro 301, Tyr 319, and Pro 320 (Figure 7). However, residues Val 300, Tyr 319, and Pro 320 are not within van der Waals contacts with tolrestat. In the ALR2 ternary complex structure, the four residues Trp 22, Trp 114, Phe 125, and Leu 301 interface with the two heterocyclic rings. The A face of the benzothiazole ring stacks against Trp 114 while the side-chain of Leu 301 apposes the B face. The phthalazinone ring is sandwiched by Trp 22 and Phe 125 (Figure 6). In the ALR1-tolrestat structure, the naphthalene ring is sandwiched by Phe 125, Trp 82, Pro 301 and Trp 220. The *N*-methylthioamide group stacks against Trp 22 and apposes Trp 114. Upon zopolrestat binding to ALR2, the side-chain of Leu 301 is displaced and together with the side-chain of Phe 125 forms a hydrophobic bridge that is involved in sequestering the inhibitor. In ALR1, the residue corresponding to Leu 301 is Pro 301 and the hydrophobic bridge between the side-chains of Leu 301 and Phe 125 of the ALR2-zopolrestat complex is missing in the ALR1-tolrestat structure. As observed in the ALR2-zopolrestat structure, the interaction between zopolrestat and the active site of FR-1 is dominated by apolar residues [15]. A comparison between the active sites of ALR2 and FR-1 shows that the conformational differences between the two enzymes are largely confined to the C-terminal loop which has been shown to be flexible [10]. However, the orientation of the bound zopolrestat in the active site of FR-1 is similar to that of ALR2 and many of the interactions between enzyme and inhibitor are conserved [15].

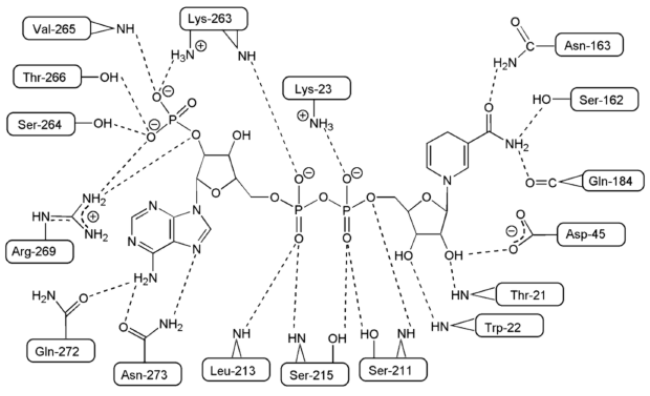

Figure 5. The coenzyme-binding site. Schematic diagram of the hydrogen bonding and salt linking interactions between ALR1 and NADPH. With the exception of Gln 272 (Glu in ALR2 and FR-1) the coenzyme-binding residues are conserved in ALR1, ALR2 and FR-1.

ARIs and clinical trials

The efficacy of several ARIs toward diabetic neuropathy and retinopathy have been examined in several clinical trials

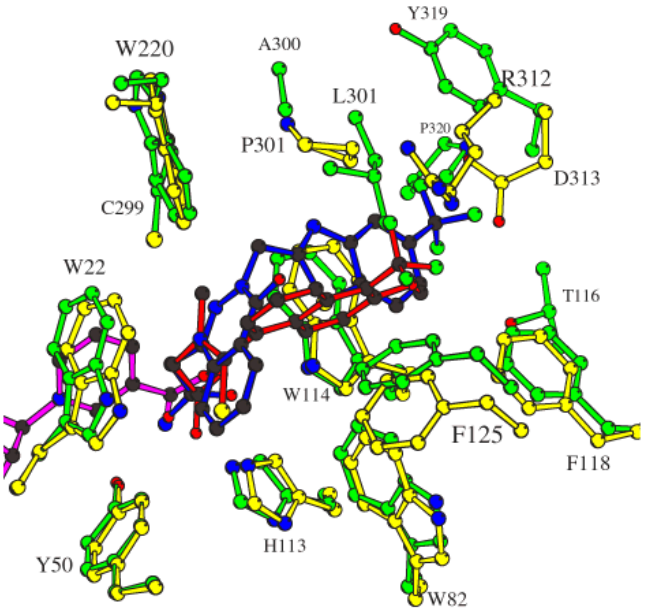

Figure 6. The inhibitor-binding site. Superimposed inhibitor-binding residues for ALR1 with bound tolrestat (amino-acid side-chains in yellow, inhibitor in red) and ALR2 with bound zopolrestat (amino-acid side-chains in green, inhibitor in blue). The inhibitor atoms are colored by type to illustrate potential hydrogen bonds (O in red, N in blue, S in yellow, F in green, C in black). For clarity, only the coenzyme molecule bound to ALR1 is shown in pink. Residues are labeled with residue type and number. The sequence numbering for aldehyde reductase (ALR1) is used [11].

in the United States (reviewed in [31] and [32]). While no ARIs have been approved, results from ongoing research into the pathogenesis of diabetic retinopathy and neuropathy should have an important impact on the design and expectations of future drug trials. For example, the Diabetes Control and Complications Trial (DCCT) showed that the incidence of retinopathy was significantly influenced by mean blood glucose levels and study participants practicing intensive as compared to conventional glycemic control experienced a marked reduction in the incidence and progression of diabetic retinopathy. The DCCT also showed that the protective effect was less noticeable if intensive control was instituted after some progression has occurred [33]. Similar results were found in a recent study of galactosemic dogs, which showed that correction of hyperglycemia through removal of dietary galactose did not stop the progressive appearance of retinal abnormalities associated with diabetic retinopathy [34]. Taken together, these studies emphasize that retinopathy follows a long term pathogenesis and that once initiated, pharmacological efforts to interfere are far less likely to be successful than prophylactic treatment prior to onset of early and perhaps irreversible tissue changes. Therefore, even if the therapeutic basis for ALR2 inhibition is valid, efficacy for a given drug might be impossible to establish if the clinical study design does not take into consideration known risk factors for retinopathy progression such as duration of diabetes, rigor of glycemic control and existence of early changes in retinal vasculature. A similar rationale applies for ARI studies to establish efficacy toward diabetic neuropathy.

In addition to these potential design flaws in prior clinical trials, failure to demonstrate inhibitor efficacy may be related to poor pharmacokinetic profiles of the investigated compounds. For example, inadequate nerve penetration almost certainly contributed to the failure of ponalrestat in clinical trials for diabetic neuropathy. In addition, unexpected toxicity was a factor leading to the termination of clinical trials of sorbinil and tolrestat [35,36]. This experience illustrates the complex array of pharmacological issues that must be addressed for successful introduction of a new ARI.

SUMMARY

In this study we have shown that the 450 and 72 fold differences in the potency of inhibition of ALR1 and ALR2 by zopolrestat and tolrestat [26], respectively, are reflected in the mode of the interaction of the inhibitors with the enzymes. The information gained from studying the hydrogen-bonding network between enzyme and inhibitor, the participation of non-conserved residues from the C-terminal loop in lining the active site pocket in ALR1 and the formation of a hydrophobic bridge over the bound inhibitor in ALR2 may be used in future efforts to design drugs based on the structure of the target enzyme.

ACKNOWLEDGEMENTS

We thank Professor Mark von Itzstein for reading the manuscript, Dr. Robin Thomson and Mr. Evans Georgalis for their assistance in preparing figures 5 and 7. This work was supported in part by research grants from Monash Research Fund, Australian Research Council and Australian National Health and Medical Research Council to OE-K, NIH grants EY05856 and EY02667 and by grants to the Department of

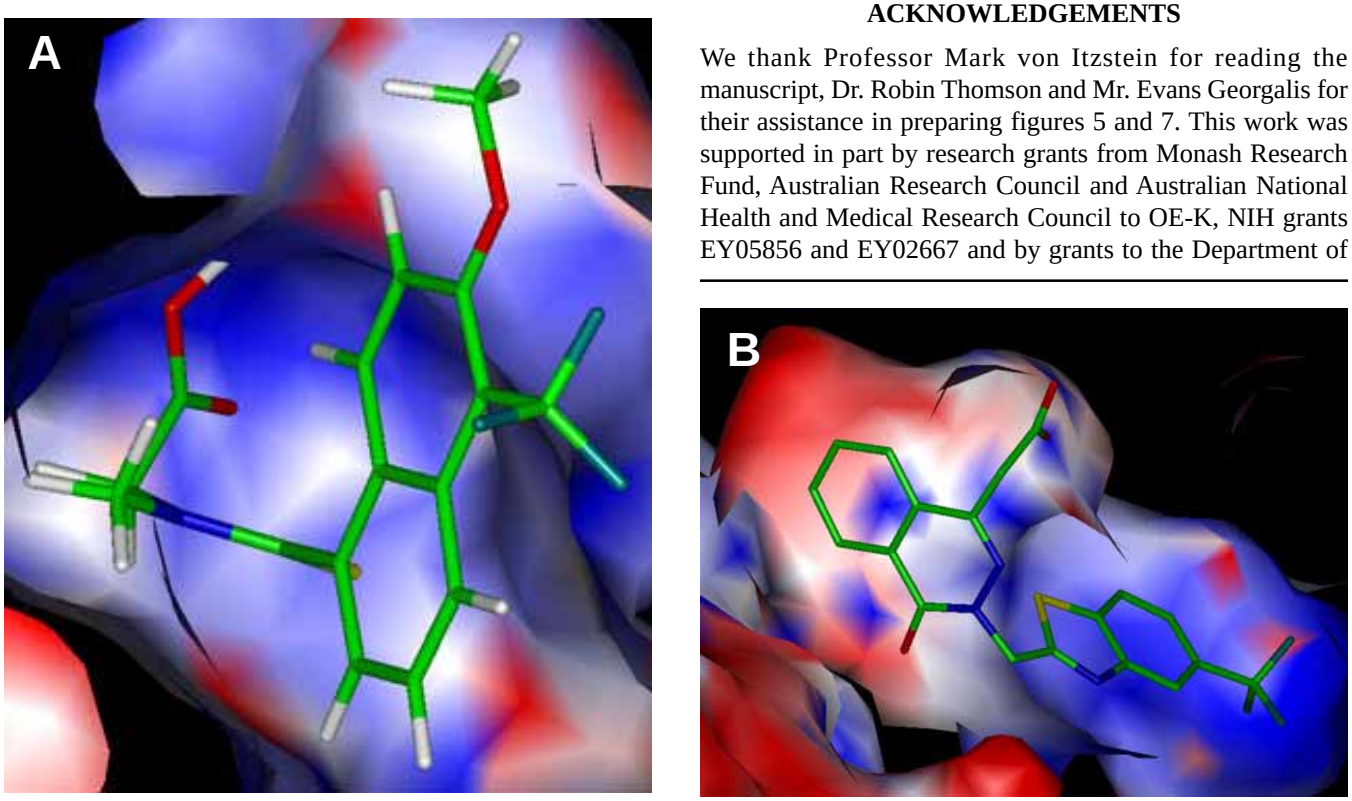

Figure 7. Surface charges of the inhibitor-binding site. Distribution of surface charges in the inhibitor-binding sites of ALR1 (A) and ALR2 (B) with the inhibitors bound. The surface of each inhibitor binding-site is colored according to the type of charge present (negative in red, positive in blue, neutral in white). The apolar surfaces interact with the hydrophobic domains of the inhibitor while the polar surfaces may engage in ionic interactions with the bound inhibitor. Excellent charge complementarity exists between the carboxylate group of the bound inhibitor and the enzyme. Figures were prepared using INSIGHT II (Biosym Technologies Inc., San Diego, CA). **(A)** ALR1. **(B)** ALR2.

Ophthalmology and Visual Sciences from Research to Prevent Blindness, Inc. to JMP. FAQ is an investigator of the Howard Hughes Medical Institute.

REFERENCES

1. Hayashi H, Fujii Y, Watanabe K, Urade Y, Hayaishi O. Enzymatic conversion of prostaglandin H2 to prostaglandin F2 alpha by aldehyde reductase from human liver: comparison to the prostaglandin F synthetase from bovine lung. J Biol Chem 1989; 264:1036-1040.

2. Jacobi GH, Moore RJ, Wilson JD. Characterization of the 3alpha-hydroxysteroid dehydrogenase of dog prostate. J Steroid Biochem 1977; 8:719-723.

3. Warren JC, Murdock GL, Ma Y, Goodman SR, Zimmer WE. Molecular cloning of testicular 20 alpha-hydroxysteroid dehydrogenase: identity with aldose reductase. Biochemistry 1993; 32:1401-1406.

4. Jez JM, Flynn TG, Penning TM. A nomenclature system for the aldo-keto reductase superfamily. Adv Exp Med Biol 1997; 414:570-600.

5. Kinoshita JH, Nishimura C. The involvement of aldose reductase in diabetic complications. Diabetes Metab Rev 1988; 4:323-337.

6. Williamson JR, Chang K, Frangos M, Hasan KS, Ido Y, Kawamura T, Nyengaard JR, van den Enden M, Kilo C, Tilton RG. Hyperglycemic pseudohypoxia and diabetic complications. Diabetes 1993; 42:801-813.

7. Lee AY, Chung SK, Chung SS. Demonstration that polyol accumulation is responsible for diabetic cataract by the use of transgenic mice expressing the aldose reductase gene in the lens. Proc Natl Acad Sci U S A 1995; 92:2780-2784.

8. Yamaoka T, Nishimura C, Yamashita K, Itakura M, Yamada T, Fujimoto J, Kokai Y. Acute onset of diabetic pathological changes in transgenic mice with human aldose reductase cDNA. Diabetologia 1995; 38:255-261.

9. Wilson DK, Bohren KM, Gabbay KH, Quiocho FA. An unlikely sugar substrate site in the 1.65 A structure of human aldose reductase holoenzyme implicated in diabetic complications. Science 1992; 257:81-84.

10. Wilson DK, Tarle I, Petrash JM, Quiocho FA. Refined 1.8 A structure of human aldose reductase complexed with the potent inhibitor zopolrestat. Proc Natl Acad Sci U S A 1993; 90:9847-9851.

11. El-Kabbani O, Green NC, Lin G, Carson M, Narayana SVL, Moore KM, Flynn TG, DeLucas LJ. Structures of human and porcine aldehyde reductase: an enzyme implicated in diabetic complications. Acta Crystallogr D Biol Crystallogr 1994; 50:859-868.

12. El-Kabbani O, Judge K, Ginell SL, Myles DA, DeLucas LJ, Flynn TG. Structure of porcine aldehyde reductase holoenzyme. Nat Struct Biol 1995; 2:687-692.

13. El-Kabbani O, Carper DA, McGowan MH, Ginell SL. Crystal structure of porcine aldehyde reductase at 2.0 A resolution: modeling an inhibitor in the active site of the enzyme. Protein and Peptide Letters 1996; 3:427-434.

14. El-Kabbani O, Carper DA, McGowan MH, Devedjiev Y, Rees-Milton KJ, Flynn TG. Studies on the inhibitor-binding site of porcine aldehyde reductase: crystal structure of the holoenzyme-inhibitor ternary complex. Proteins 1997; 29:186-192.

15. Wilson DK, Nakano T, Petrash JM, Quiocho FA. 1.7 A structure of FR-1, a fibroblast growth factor-induced member of the aldo-keto reductase family, complexed with coenzyme and inhibitor. Biochemistry 1995; 34:14323-14330.

16. Hoog SS, Pawlowski JE, Alzari PM, Penning TM, Lewis M. Three-dimensional structure of rat liver 3 alpha-hydroxysteroid/dihydrodiol dehydrogenase: a member of the aldo-keto reductase superfamily. Proc Natl Acad Sci U S A 1994; 91:2517-2521.

17. Lui SQ, Bhatnagar A, Srivastava SK. Bovine lens aldose reductase. pH-dependence of steady-state kinetic parameters and nucleotide binding. J Biol Chem 1993; 268:25494-25499.

18. Bohren KM, Grimshaw CE, Lai CJ, Harrison DH, Ringe D, Petsko GA, Gabbay KH. Tyrosine-48 is the proton donor and histidine-110 directs substrate stereochemical selectivity in the reduction reaction of human aldose reductase: enzyme kinetics and crystal structure of the Y48H mutant enzyme. Biochemistry 1994; 33:2021-2032.

19. Tarle I, Borhani DW, Wilson DK, Quiocho FA, Petrash JM. Probing the active site of human aldose reductase. Site-directed mutagenesis of Asp-43, Tyr-48, Lys-77 and His-110. J Biol Chem 1993; 268:25687-25693.

20. Pawlowski JE, Penning TM. Overexpression and mutagenesis of cDNA for rat liver 3 alpha-hydroxysteroid/dihydrodiol dehydrogenase. Role of cysteines and tyrosines in catalysis. J Biol Chem 1994; 269:13502-13510.

21. Kubiseski TJ, Hyndman DJ, Morjana NA, Flynn TG. Studies on pig muscle aldose reductase. Kinetic mechanism and evidence for a slow conformational change upon coenzyme binding. J Biol Chem 1992; 267:6510-6517.

22. Davidson WS, Flynn TG. Kinetics and mechanism of aldehyde reductase from pig kidney. Biochem J 1979; 177:595-601.

23. Barski OA, Gabbay KH, Bohren KM. The C-terminal loop of aldehyde reductase determines the substrate and inhibitor specificity. Biochemistry 1996; 35:14276-14280.

24. Ehrig T, Bohren KM, Prendergast FG, Gabbay KH. Mechanism of aldose reductase inhibition: binding of NADP+/NADPH and alrestatin-like inhibitors. Biochemistry 1994; 33:7157-7165.

25. Carper DA, Hohman TC, Old SE. Residues affecting the catalysis and inhibition of rat lens aldose reductase. Biochim Biophys Acta 1995; 1246:67-73.

26. Barski OA, Gabbay KH, Grimshaw CE, Bohren KM. Mechanism of human aldehyde reductase: characterization of the active site pocket. Biochemistry 1995; 34:11264-11275.

27. Kubiseski TJ, Flynn TG. Studies on human aldose reductase. Probing the role of 268 by site-directed mutagenesis. J Biol Chem 1995; 270:16911-16917.

28. Wirth HP, Wermuth B. Immunohistochemical localisation of aldehyde and aldose reductase in human tissues. Prog Clin Biol Res 1985; 174:231-239.

29. Sato S, Kador PF. Inhibition of aldehyde reductase by aldose reductase inhibitors. Biochem Pharmacol 1990; 40:1033-1042.

30. Wermuth B. Aldo-keto reductases. Prog Clin Biol Res 1985; 174:209-230.

31. Krans HM. Recent clinical experience with aldose reductase inhibitors. Diabet Med 1993; 10:44S-48S.

32. Pfeifer MA, Schumer MP, Gelber DA. Aldose reductase inhibitors: the end of an era or the need for different trial designs? Diabetes 1997; 46 Suppl 2:S82-S89.

33. The effect of intensive diabetes treatment on the progression of diabetic retinopathy in insulin-dependent diabetes mellitus. The Diabetes Control and Complications Trial Research Group. Arch Ophthalmol 1995; 113:36-51.

34. Engerman RL, Kern TS. Retinopathy in galactosemic dogs continues to progress after cessation of galactosemia. Arch Ophthalmol 1995; 113:355-358.

35. A randomized trial of sorbinil, an aldose reductase inhibitor, in diabetic retinopathy. Sorbinil Retinopathy Trial Research Group. Arch Ophthalmol 1990; 108:1234-1244.

36. Foppiano M, Lombardo G. Worldwide pharmacovigilance systems and tolrestat withdrawal. Lancet 1997; 349:399-400.

37. Kraulis PJ. MOLSCRIPT: a program to produce both detailed and schematic plots of protein structures. Journal of Applied Crystallography 1991; 24:946-950.